Dependence of birefringence on elliptical-hole orientation in photonic crystal fibers*

TAN Xiao-ling(谭晓玲), **ZHANG Ling-fen**(张玲芬)**, **JIANG Wen-xiao**(蒋文晓), **ZHANG Qi**(张琪), **and ZHOU Jun**(周骏)

Faculty of Science, Ningbo University, Ningbo 315211, China

(Received 19 September 2012)

In this paper, the dependence of birefringence on the orientation of elliptical holes in triangular-lattice elliptical-hole photonic crystal fibers (PCFs) is investigated numerically. A resonant enhancement of birefringence between the anisotropic lattice arrangement and oriented elliptical holes is observed, and the birefringence varies periodically with the elliptical-hole orientation. When the major axes of adjacent elliptical holes are parallel, the birefringence approaches the maximum. Based on the numeric analysis, a novel highly birefringent PCF is proposed, and the maximum modal birefringence of 0.086 is achieved.

Document code: A **Article ID:** 1673-1905(2013)01-0061-4

DOI 10.1007/s11801-013-2355-5

In recent years, photonic crystal fibers (PCFs) have attracted great attentions for their unique features, such as endless single-mode operating[1], tailorable dispersion[2,3], high nonlinearity[4] and high birefringence. One possible use of highly birefringent (Hi-Bi) PCFs is as polarization-maintaining fibers, which can eliminate the influence of polarization mode dispersion and stabilize the operation of optical devices in high bit rate communication systems and fiber loops for gyroscopes. However, in conventional polarization-maintaining fibers, such as PANDA[5] and bow-tie fibers[6], the modal birefringence induced by stress near the core region is about 5×10^{-4}, which can not satisfy the potential uses in novel optical devices.

As for PCFs, benefiting from the design flexibility and higher index contrast, the modal birefringence of 10^{-2} can be reached, which is roughly two orders of magnitude larger than that of the conventional fibers. To date, many approaches have been explored for achieving Hi-Bi PCFs. Moreover, the Hi-Bi PCFs using soft and silica glasses were successfully developed[7,8]. Besides imposing an external stress to induce an asymmetric transverse index profile[9, 10] by elasto-optical effect, especially in large-mode-area PCFs, the most typical method is to break the regular geometry of the fiber core or the air-hole cladding, which can lead to much larger birefringence than the stress-induced ones[11]. As for the asymmetric fiber cores, various Hi-Bi PCFs have been proposed, for example, using two enlarged central holes around the central core[12] and adding large air holes outside the cladding[13]. Another effective way is to replace the circular holes with anisotropy shape ones, such as elliptical holes[14]. Most often, combination of the two mechanisms can also lead to high modal birefringence[15]. In Ref.[15], a rectangular lattice elliptical-hole fiber was proposed, which used an asymmetric core and elliptical holes in the whole region, and it exhibits a great promise to realize ultrahigh birefringence. However, in these literatures, elliptical holes were typically placed along a fixed direction, and few reports have put on the dependence of birefringence on the orientation of elliptical air holes. So in this paper, we restrict our concentration to this issue and analyze it by fundamental space-filling modes (FSMs) indirectly. Moreover, based on the analysis, a novel microstructured optical fiber (MOF) with the maximum modal birefringence of 0.086 is proposed, to the best of our knowledge, which is the highest value now.

The cross section of Hi-Bi PCF and triangular-lattice arrangement of elliptical holes are shown in Fig.1. It is characterized by the following parameters. The ellipticity is $\eta = b/a$, where b and a are the lengths of the semi-major axis and semi-minor axis, respectively. The lattice pitches along horizontal and vertical directions are $\ddot{E}_x$ and $\ddot{E}_y$, respectively, and

* This work has been supported by the Ningbo Natural Science Foundation (No. 2011A61090) , and the K. C. Wong Magna Fund in Ningbo University.

** E-mail: zhanglingfen@nbu.edu.cn

for this regular hexagonal lattice, the relationship of $\Lambda_y = 2\Lambda_x\cos(\pi/6)$ exists between the two lattice pitches. The air-filling factor is $A=2\pi ab/\Lambda_x\Lambda_y$. θ is the rotated angle from major axis to the vertical direction, that is, when $\theta = 0$, the arrangement of the elliptical holes is the typical schematic of PCFs without squeezed effect as mentioned before. In addition, the refractive index of background silica is taken to be n=1.45, and the material dispersion is neglected for convenience.

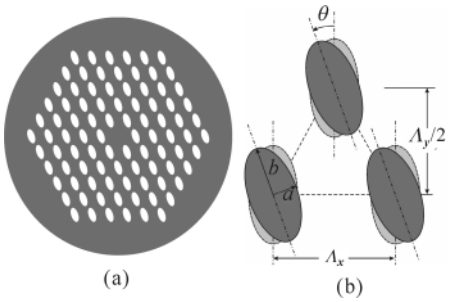

Fig.1 Schematic diagrams of (a) cross section of Hi-Bi PCF and (b) triangular-lattice arrangement of elliptical holes with rotated angle θ

In an elliptical-hole PCF, the modal birefringence results from the anisotropy of cladding in two orthogonally polarized directions, and strongly depends on the degree of mode penetration into cladding. In this case, the birefringence of FSMs indirectly indicates the maximum possible modal birefringence. So it is convenient to analyze the birefringence of FSMs for different rotated angles regardless of the core shapes. The birefringence of FSMs is expressed by $B_{FSM}=|n^y_{FSM}-n^x_{FSM}|$, where n^y_{FSM} and n^x_{FSM} are the effective indices of y-polarized and x-polarized FSMs, respectively. A free software package of the plane-wave expansion method is employed to calculate B_{FSM} for the periodic-structured cladding. At a given propagation constant, FSMs refer to the lowest Bloch states at the point of Γ, so the effective indices of FSMs can be obtained conveniently by the calculation of only one k-point (0, 0, k_z), and enough accuracy is guaranteed by setting a resolution of 512×512 in an elliptical-hole unit cell. Moreover, as we know, B_{FSM} increases with wavelength for asymmetric cladding. Therefore, we only examine the value of B_{FSM} at the normalized wavelength λ/Λ_x=1.55.

Fig.2 shows the birefringence of FSMs as a function of rotational angle of θ at three different ellipticities of 2, 2.5 and 3 when A = 0.2. We find that the birefringence of FSMs varies periodically with the elliptical-hole orientation, and the period of 60° can be observed. The maximum B_{FSM} occurs when θ = 30° and 90°, and it is easy to predict the other four maximum points according to the six-fold rotational symmetry of triangular lattice. At these rotational angles, the major axes of adjacent elliptical holes are parallel, while at the angles of θ = 0° and 60° where the minimum B_{FSM} occurs, the minor axes of adjacent elliptical holes are parallel. In addition, it exhibits that the maximum increase of B_{FSM} varies with air-hole ellipticities, i.e., the larger the ellipticity is, the more obvious the increase becomes. Seen from Fig.2, the maximum increase of B_{FSM} is 0.97×10^{-3}, 1.73×10^{-3} and 2.84×10^{-3} for ζ = 2, 2.5 and 3, respectively.

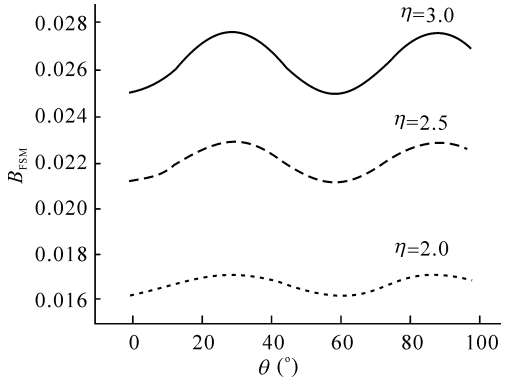

Fig.2 Birefringence of FSMs as a function of air-hole rotated angle θ when A=0.2

Besides the enhanced birefringence of FSMs changing with air-hole ellipticity, we also investigate it for different air-filling factors. Fig.3 shows the holes-oriented dependence of B_{FSM} at different ellipticities (η =2, 2.5 and 3) when A=0.1 and 0.3, respectively. The increase of B_{FSM} is more obvious with air-filling factor increasing. For example, B_{FSM} increases by 1.5×10^{-2} for ζ = 3 and A = 0.3, which is approximately two orders of magnitude larger than that of A = 0.1. Fig.4 exhibits the absolute magnetic field distribution $|\boldsymbol{H}|$ corresponding to the minimum and maximum values of B_{FSM}, i.e., at θ=0° and 90°, respectively. It is clearly seen that the amplitude of $|\boldsymbol{H}|$ at θ =90° increases much larger than that of θ=0° with the increase of B_{FSM} correspondingly. Finally, the modal birefringence is checked again at λ/Λ_x=1.55 for the typical structure of elliptical-hole PCFs, where the core is also formed by an absence of an elliptical hole. The modal birefringence is enhanced to 2.45×10^{-2} at θ=90° from 1.67×10^{-2} at θ = 0°.

From the above analyses, we know that B_{FSM} varies periodically with the orientation of elliptical air holes regardless of ellipticities or air-filling factors, and the maximum B_{FSM} occurs when the major axes of elliptical holes are parallel. For the triangular-lattice PCFs, as the conventional circular air holes are replaced by elliptical holes and the six-fold rotational symmetry degenerates to C_{2V}, the structure of the triangular-lattice arrangement is asymmetric in two orthogonal major-axis and minor-axis directions. So the birefringence of FSMs is influenced by both intrinsic lattice asymmetry and anisotropy of elliptical holes. When the major axes of

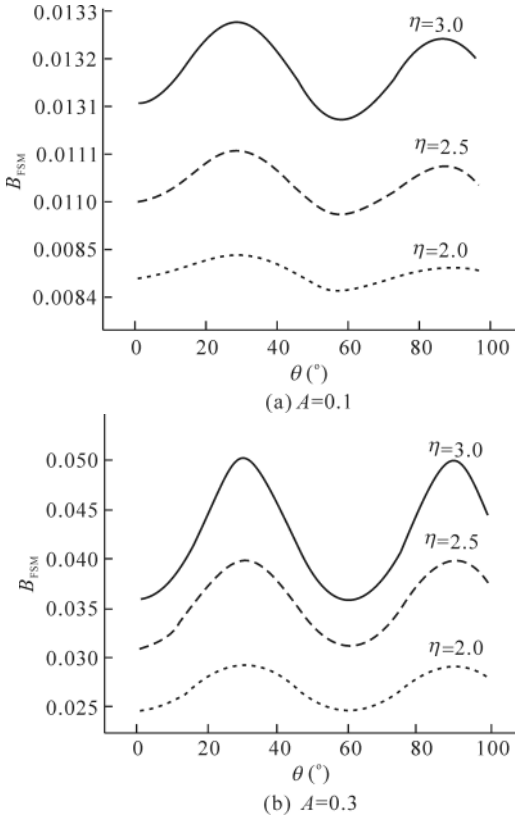

Fig.3 Birefringence of FSMs as a function of air-hole rotated angle θ at different ellipticities

elliptical holes are parallel, a resonant enhancement appears between the two effects induced by lattice asymmetry and anisotropy of elliptical holes, therefore, B_{FSM} reaches the maximum value. However, in some rotated angles (e.g., $\dot{e} = 0^{o}$), the two anisotropic effects counteract each other, and B_{FSM} reaches the minimum value.

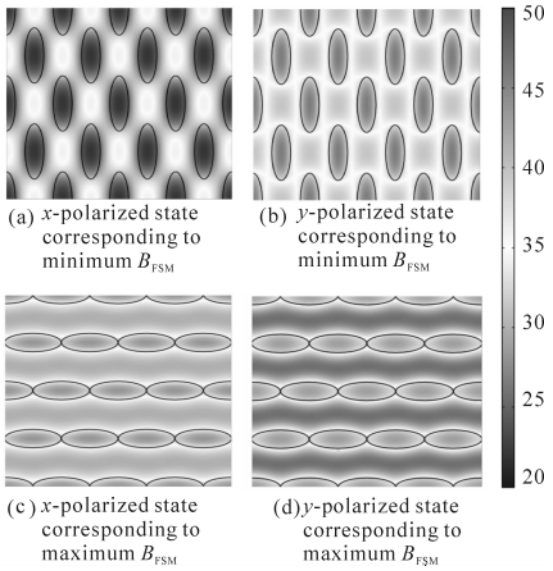

Fig.4 Magnetic field distributions of FSMs when η =3 and A=0.3

In order to verify our view further, we break the relationship of $\ddot{E}_y = 2\ddot{E}_x\cos(\pi/6)$ to make the lattice squeezed or elongated. The squeezed ratio between horizontal and vertical lattice pitches is expressed by $\zeta=\ddot{E}_y / \ddot{E}_x$. Fig.5 plots the variation of B_{FSM} with normalized wavelength of $\ddot{e}/\ddot{E}_x$ when $\dot{e}$=0° and $\dot{e}$=90°, and the ellipticity and air-filling factor are fixed at 2.5 and 3, respectively. From the comparison of the two typical elliptical-hole orientations, it indicates that the enhancement effect of B_{FSM} becomes more obvious as the squeezed ratio increasing. It should be noted that when ζ=1, B_{FSM} for the two orientations overlap each other, that is to say B_{FSM} at $\dot{e}$ = 90° isn't enhanced any more. Actually, in this case, the triangular-lattice arrangement of air holes evolves into square-lattice arrangement, and structural asymmetries caused by two lattice arrangements are the same, so the enhancement of B_{FSM} at $\dot{e}$ = 90° isn't observed (although counteraction effect maybe happen for other directions). Furthermore, owing to the existence of the counteraction effect at $\dot{e}$=0°, B_{FSM} decreases slightly as the squeezed ratio increases, which can be clearly seen from the comparison in Fig.5, while it greatly increases with squeezed ratio increasing at $\dot{e}$=90°, which also reflects the existence of oriented enhancement and counteraction between two asymmetric geometries from a view of the other side.

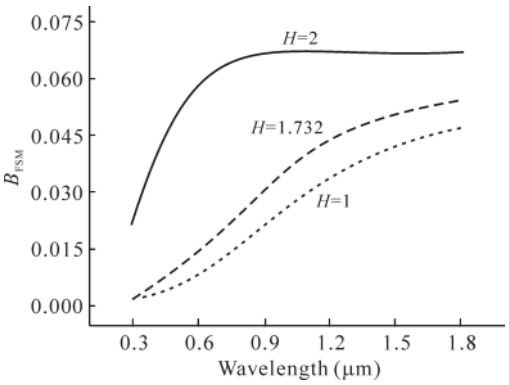

Fig.5 B_{FSM} versus normalized wavelength of λ/Λ_x at different squeezed ratios of 1, 1.732 and 2 for PCFs with elliptical holes arranged at θ = 0 and π/2

From the above analyses, we know that the difference in two orthogonal directions reaches the maximum value when the major axes of elliptical holes are parallel, and in this case, we also find that B_{FSM} increases with squeeze ratio reducing when elliptical-hole shape is kept the same. Therefore, a novel Hi-Bi microstructured optical fiber (MOF) using flat elliptical holes as fiber cladding is proposed. Its schematic diagram of cross section is shown as Fig.6, where the cladding of MOF is composed of two kinds of tightly flat elliptical air holes. Eight larger elliptical holes are arranged along vertical direction, and two small elliptical holes are horizontally

placed around the fiber core. This MOF is characterized by the following parameters. For larger air holes, holes space is $\ddot{E}_y$, the lengths of major axis and the minor axis are L and S, respectively, ellipticity is L/S=14, and L=13$\ddot{E}_y$. For two small elliptical air holes, holes space is $\ddot{E}_x$=8$\ddot{E}_y$, the lengths of major axis and the minor axis are L' and S', respectively, ellipticity is L/S=10, and L'=5$\ddot{E}_y$. The solid fiber core is defined by $\ddot{E}$=3$\ddot{E}_y$. The squeezed ratio can be considered as H=$\ddot{E}_y$ / L=1/13.

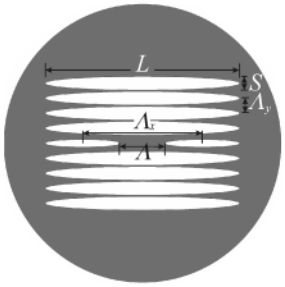

Fig.6 Cross section of the flat elliptical-hole microstructured optical fiber

Fig.7 shows the modal birefringence of the two orthogonally polarized fundamental modes HE^x_{11} and HE^y_{11}, respectively. The maximum B of 0.086 is achieved at $\ddot{e}/\ddot{E}$=1.17. The intensity distributions of the two orthogonally polarized fundamental modes are plotted in Fig.8, and they are confined well in the fiber core. Moreover, it is confirmed that the confinement loss can be reduced significantly by adding more air holes around the highly flat elliptical holes, and the modal birefringence can be increased further using smaller $\ddot{E}_y$ based on this kind of flat elliptical-hole MOFs.

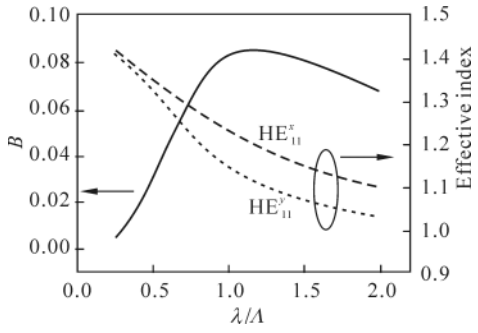

Fig.7 Modal birefringence and effective index of the two orthogonally polarized fundamental modes of HE^x_{11} and HE^y_{11}, respectively

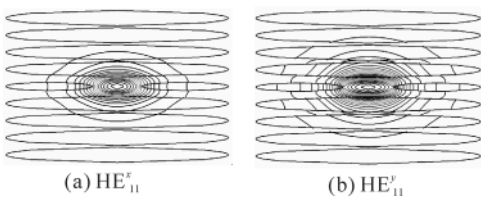

Fig.8 Intensity distributions of the two orthogonally polarized fundamental modes for λ/Λ=1.17

In this paper, the dependence of birefringence on the orientation of the elliptical holes in triangular-lattice elliptical-hole PCFs is investigated numerically, and a resonant enhancement of birefringence is observed. For PCFs with elliptical-hole cladding, the birefringence varies periodically for the enhancement or counteraction effect between the anisotropic lattice arrangement and orientation of elliptical holes in some directions. When the major axes of adjacent elliptical holes are parallel, birefringence of fiber cladding approaches the maximum. Moreover, the larger the ellipticity and air-filling ratio are, the larger the birefringence is. Finally, we propose a novel MOF with highly flat elliptical-hole cladding, and the modal birefringence of 0.086 is realized. However, we believe that the modal birefringence could be enhanced further based on our analysis.

References

[1] T. A. Birks, J. C. Knight and P. J. Russell, Opt. Lett. **22**, 961 (1997).

[2] J. C. Knight, J. Arriaga, T. A. Birks, A. Ortigosa-Blanch, W. J. Wadsworth and P. J. Russell, IEEE Photon. Technol. Lett. **12**, 807 (2000).

[3] W. H. Reeves, J. C. Knight, P. J. Russell and P. J. Roberts, Opt. Express **10**, 609 (2002).

[4] J. K. Ranka, R. S. Windeler and A. J. Stentz, Opt. Lett. **25**, 25 (2000).

[5] T. Hosaka, K. Okamoto, T. Miya, Y. Sasaki and T. Edahiro, Electron. Lett. **17**, 530 (1981).

[6] R. D. Birch, D. N. Payne and M. P. Varnham, Electron. Lett. **18**, 1036 (1982).

[7] R. Buczynski, I. Kujawa, D. Pysz, T. Martynkien, F. Berghmans, H. Thienpont and R. Stepien, Appl. Phys. B **99**, 13 (2010).

[8] F. Beltrán-Mejía, G. Chesini, E. Silvestre, A. K. George, J. C. Knight and C. M. Cordeiro, Opt. Lett. **35**, 544 (2010).

[9] Z. Zhu and T. G. Brown, Opt. Lett. **28**, 2306 (2003).

[10] T. Schreiber, H. Schultz, O. Schmidt, F. Röser, J. Limpert and A. Tünnermann, Opt. Express **13**, 3637 (2005).

[11] B. Sun, M. Y. Chen, R. J. Yu, Y. K. Zhang and J. Zhou, Optoelectronics Letters **7**, 253 (2011).

[12] S. S. Zhang, W. G. Zhang, Z. L. Liu and X. L. Li, Journal of Optoelectronics • Laser **22**, 685 (2011). (in Chinese)

[13] C. Wu, J. Li, X. Feng, B. O. Guan and H. Y. Tam, J. Lightwave Technol. **29**, 943 (2011).

[14] Y. Yue, G. Y. Kai, Z. Wang, T. T. Sun, L. Jin, Y. F. Lu, C. S. Zhang, J. G. Liu, Y. Li, Y. G. Liu, S. Z. Yuan and X. Y. Dong, Opt. Lett. **32**, 469 (2007).

[15] I. Kujawa, R. Buczynski, T. Martynkien, M. Sadowski, D. Pysz, R. Stepien, A.Waddie and M. R. Taghizadeh, Opt. Fiber Technol. **18**, 220 (2012).